Electric and magnetic properties of the four most stable CHNO isomers from ab initio CCSD(T) studies

Mirjana Mladenović, Mohamed Elhiyani, and Marius Lewerenz

Additional information on J. Chem. Phys.

Electric and magnetic properties of the four most stable CHNO isomers from *ab initio* CCSD(T) studies

Mirjana Mladenović,[a)] Mohamed Elhiyani,[b)] and Marius Lewerenz[c)]

Laboratoire Modélisation et Simulation Multi Echelle, Université Paris-Est, MSME FRE3160 CNRS,
5 bd Descartes, 77454 Marne la Vallée, France

Electric and magnetic properties obtained from CCSD(T)/(aug-)cc-pCVXZ (X=T, *Q*, or 5) electronic structure calculations are reported for isocyanic acid, HNCO, cyanic acid, HOCN, fulminic acid, HCNO, and isofulminic acid, HONC, in their ground electronic states. Comparison of the theoretical results with the available experimentally derived values shows very satisfactory agreement. The new data should be helpful for the identification of these molecules due to characteristic hyperfine structure patterns in their microwave spectra. A brief discussion of the electronic structure properties, based on the electric field gradients, Mulliken population analysis of the total electron density, and molecular orbitals, is provided for the four CHNO isomers and the related HCN/HNC system. © *2009 American Institute of Physics*. [DOI: 10.1063/1.3173275]

I. INTRODUCTION

Rotational (microwave) spectroscopy is a powerful means of studying free molecules. Microwave measurements yield precise data on rotational and centrifugal distortion constants, as well as, e.g., dipole moments and nuclear quadrupole coupling constants. These quantities allow, in return, the derivation of various types of molecular information, such as the equilibrium geometry and electronic structure. Microwave data for a molecule of interest may additionally lead to conclusions about the rotational-vibrational and/or rotational-electronic coupling(s) and to estimations of the related interaction parameters.

Rotational transitions can exhibit hyperfine structure, governed by the spin angular momentum. Characteristic hyperfine structure patterns can be a key element in the identification of unstable or low abundance species whose rotational spectra are incomplete or masked by overlap with other spectra, a frequent situation in astronomical surveys. The CHNO isomers built from the four most important atoms of biochemistry are of prime interest in this context. For molecules of zero electronic spin and orbital angular momentum in a ground electronic state, Flygare[1] discussed in detail the important magnetic interactions, measurable by microwave resonance techniques. Rotational-electronic interactions, arising from the intrinsic nonseparability of electronic and rotational motions, contribute to the rotational magnetic moment. In rotating molecules, the rotational magnetic field due to the motion of nuclear and electronic charges may give rise to nuclear spin-rotation coupling and magnetic shielding. Magnetic field-electronic interactions in the presence of nonzero external magnetic fields contribute to molecular *g* values and magnetic susceptibilities (the ro-

tational molecular Zeeman effect). The relation between the spin-rotation and magnetic shielding tensors and the relation between the molecular magnetic moment (*g*) and magnetic susceptibility tensors have been established by Flygare.[1,2]

Atomic nuclei with nuclear spin $I \geq 1/2$ possess nonzero magnetic dipole moments and, thus, nonzero spin-rotation coupling constants. Atomic nuclei with nuclear spin $I \geq 1$ are quadrupolar, due to a nonzero electric quadrupole moment (resulting from a nonspherical charge density distribution within the nucleus), and are involved in nuclear quadrupole interactions.[3] The proton is, e.g., a spin-1/2 fermion and the deuteron a spin-1 boson. In other words, whereas hydrogen and deuterium nuclei both have a nonzero nuclear spin-rotation tensor, only deuterium possesses nonzero nuclear quadrupole coupling constants. Elongated nuclei possess positive quadrupole moments (e.g., ^{14}N and D) and flattened nuclei negative quadrupole moments (e.g., ^{17}O).

The hyperfine coupling constants depend on the electric quadrupole moment and/or magnetic dipole. Hyperfine splittings due to nuclear quadrupole moments are generally more prominent than those due to magnetic moments. The quadrupolar splittings are usually well resolved. The characteristic spectral fingerprint of the $J=0 \rightarrow 1$ transition in molecules with a quadrupolar $I=1$ nucleus, such as ^{14}N, is a group of three well resolved components with a 1:5:3 intensity ratio. Spin-rotation interaction typically leads to very small splittings below the resolution of many microwave spectrometers and often appears as effective line broadening. Hyperfine coupling constants and their dependence on the molecular structure are considered in great detail in the classical microwave spectroscopy book by Townes and Schawlow.[3]

The nuclear quadrupole moment interacts with the second derivative of the electrostatic potential, i.e., with the electric field gradient. Since the nuclear electric field gradient is an inner shell molecular property, decreasing with the third power of the distance from the nucleus,[3] significant contributions from electron correlation may be expected

---

a)Author to whom correspondence should be addressed. Electronic mail: mladenov@univ-mlv.fr.
b)Electronic mail: elhiyani@univ-mlv.fr.
c)Electronic mail: lewerenz@univ-mlv.fr.

from the theoretical point of view. To obtain reliable results when calculating the electric field gradients, it is hence necessary to have a basis set which describes the core electrons as well as the valence electrons properly (at least for the nucleus in question), in addition to an adequate treatment of electron correlation. The nuclear quadrupole coupling constants obtained from the related electric field gradients may thus serve as a sensitive indicator of the quality of the wave function near the nuclei of interest.

Hyperfine interaction constants are nowadays obtainable by means of modern *ab initio* electronic structure methods, which employ quantum-mechanical (first-order and second-order) perturbation theory to compute the necessary quantities. Theoretical results can assist experimental work in their attempts to assign or confirm observed spectra, and in the search for unobserved molecular species.

In the present study, we concentrate on the hyperfine structure parameters of the four most stable CHNO isomers. These are isocyanic acid, HNCO, cyanic acid, HOCN, fulminic acid, HCNO, and isofulminic acid, HONC. The four CHNO molecules were recently subjected to extensive theoretical *ab initio* investigations concerning their equilibrium structures and energetics.[4,5] There, we found at the all electron CCSD(T) level of theory in combination with large correlation consistent bases that HOCN, HCNO, and HONC lie 24.5 kcal/mol (8577 cm^{-1}), 70.0 kcal/mol (24 467 cm^{-1}), and 84.2 kcal/mol (29 464 cm^{-1}) above the most stable HNCO molecule. Harmonic frequencies computed at the CCSD(T) level of theory were reported for HNCO, HOCN, and HCNO in Ref. 4 and for HONC in Ref. 5. Key rovibrational spectroscopic features resulting from a large amplitude bending vibration were also discussed.[5] Additional information concerning the electric and magnetic features of the CHNO family is provided in this work. The CHNO isomers possess large electric dipole moments of approximately 1–4 D;[4,6,7] their more precise values are found in the present report. This high polarity of the CHNO family facilitates their spectroscopic observation.

The CHNO molecules have been of longstanding chemical interest since the 16th century.[8] The first microwave observation of isocyanic acid due to Jones *et al.*[9] goes back to 1950. Since then, the spectroscopic constants reported for HNCO, in addition to the effective rotational parameters,[10] also include the dipole moments, nuclear quadrupole interaction constants for the ^{14}N, D, and ^{17}O nuclei, as well as the spin-rotation interaction strength constants.[11–14] The microwave spectra of fulminic acid and several of its isotopic species were observed for the first time by Winnewisser and Bodenseh,[15] who also derived the oxygen nuclear quadrupole constant. The nitrogen and deuterium quadrupole constants of HCNO were obtained by Hüttner *et al.*[16] in their study of the rotational Zeeman effect in HCNO and DCNO. Takashi *et al.*[17] reported precise measurements of the dipole moment of HCNO and its vibrational dependence. Regarding the HOCN and HONC molecules, only two reports appear in the literature, both of them very recent studies. Brünken *et al.*[18] and McCarthy and Thaddeus[19] measured gas phase rotational spectra in the centimeter and millimeter regions of HOCN

and HONC, respectively, deriving for the first time precise ground state spectroscopic constants for these two molecules.

The four CHNO isomers are of considerable astrophysical interest, and are expected, most prominently HNCO, to participate in interstellar chemistry.[20] Isocyanic acid was first identified by Buhl *et al.*[21] in the galactic center and by Rieu *et al.*[22] in external galaxies. Very recently, Knez *et al.*[23] made the first infrared observation of interstellar HNCO (125 lines of the ν_4 band). Interstellar fulminic acid was detected for the first time by Marcelino *et al.*[24] in dark clouds. After a first tentative detection of HOCN in Sgr B2(OH),[18] Brünken *et al.*[25] were able to identify interstellar HOCN in several additional regions in galactic center molecular clouds. Note also that Turner[26] found detailed modeling of the hyperfine structure relevant for the determination of accurate abundances of quadrupolar species (e.g., those containing ^{14}N and/or D) in astronomical sources.

Previous theoretical work on the CHNO isomers has addressed the equilibrium structure, energetics, isomerization paths, and effective rotational parameters, as reviewed before.[4–6] Regarding earlier theoretical results for electric and magnetic properties, attempts can be mentioned to calculate the electric field gradients of HNCO at the Hartree–Fock level,[27] several post-Hartree–Fock levels,[28,29] and by means of density functional methods,[30] used also to calibrate nuclear quadrupole moments on experimental data.[28–30] To the best of our knowledge, no other *ab initio* calculations on electric field gradients and spin-rotation constants are available in the literature for the CHNO family.

II. COMPUTATIONAL DETAILS

Electron correlation has been accounted for by coupled cluster calculations CCSD(T) with full iterative treatment of single and double excitations and perturbative correction for triple excitations. Dunning's correlation consistent polarized core-valence cc-pCVXZ and singly augmented aug-cc-pCVXZ basis sets[31,32] for X=T, Q, and 5 were employed. The CCSD(T) values for the electric field gradients, dipole moments, quadrupole moments, and nuclear spin-rotation coupling constants were computed including all electrons in the correlation treatment.

The Mainz-Austin-Budapest version of the ACES II program package[33,34] was used in the present work. The electric field gradient tensors and other electric properties were computed by means of the analytical first-order properties algorithm, whereas the approach based on the gauge-including atomic orbital ansatz was employed for the determination of the nuclear spin-rotation tensors.[35,36]

III. EQUILIBRIUM GEOMETRY

The structural parameters used in the present work for the CHNO isomer family are depicted in Fig. 1. They were obtained in the all electron CCSD(T)/cc-pCV5Z, CCSD(T)/cc-pCVQZ, and CCSD(T)/cc-pCVTZ calculations reported previously.[4,5]
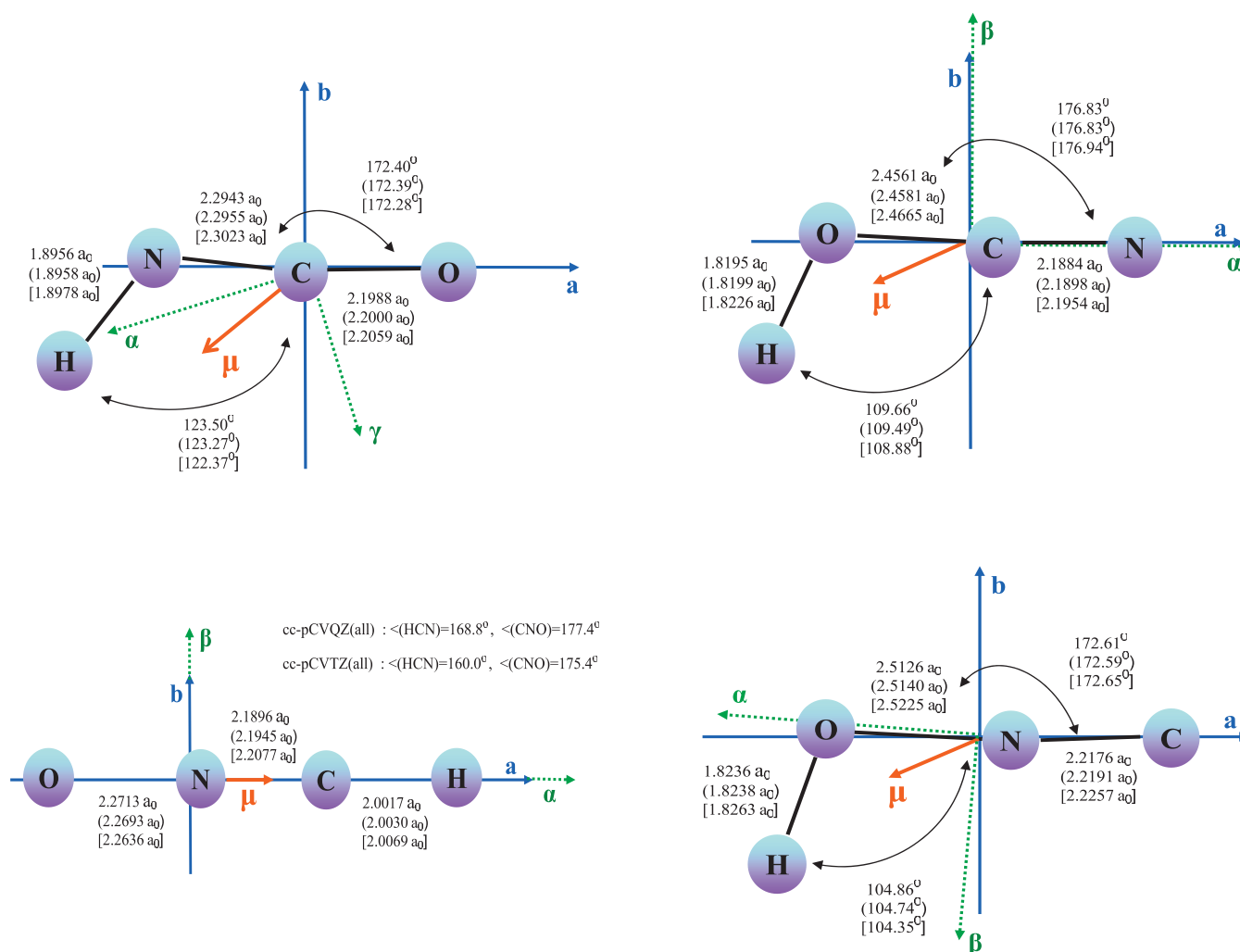
FIG. 1. Structural parameters of HNCO, HOCN, HCNO, and HONC from the CCSD(T)/cc-pCV5Z, CCSD(T)/cc-pCVQZ (in parentheses), and CCSD(T)/cc-pCVTZ (in square brackets) calculations. The principal inertial axes a, b and the principal nuclear quadrupole axes α, β, γ of the tensor $\chi(^{14}N)$ are shown in addition to the dipole moment vector μ.

The three nonlinear HXYZ molecules possess a nearly linear heavy-atom XYX chain, described by $\angle(XYX) = 172° - 177°$ in Fig. 1. With the hydrogen atom positioned off this axis, the two moments of inertia, I_b and I_c, are large and similar, being also much larger than the small moment of inertia I_a, such that $A > B \approx C$ holds for the rotational constants. In consequence, HNCO, HOCN, and HONC are very nearly prolate symmetric tops, with values for Ray's asymmetry parameter $\kappa = (2B - A - C)/(A - C)$ of -0.9994 (HONC), -0.9995 (HOCN), and -0.9997 (HNCO).

For fulminic acid, a linear equilibrium structure depicted in Fig. 1 is obtained from the CCSD(T)/cc-pCV5Z(all) calculation. Note, however, that HCNO is nonlinear at the CCSD(T)/cc-pCVXZ(all) level for $X < 5$, possessing a small barrier to linearity of 2.2 cm^{-1} and 23.4 cm^{-1} for $X = 4$ and $X = 3$, respectively.[4] For the singly augmented aug-cc-pCVXZ correlation consistent set of basis functions, HCNO is found to be linear already at the quadruple ζ level, with structural parameters $[r_e(HC), r_e(CN), r_e(NO]$ given by $[2.0026a_0, 2.1912a_0, 2.2739a_0]$.[5] For the aug-cc-pCV5Z basis, we previously obtained $[2.0020a_0, 2.1897a_0, 2.2723a_0]$.[5] We refer to Refs. 4 and 5 for more details on converging the equilibrium structure of HCNO to the linear arrangement.

The CHNO isomer family is isoelectronic with, e.g., carbon dioxide, CO_2, hydrogen azide, HN_3, nitrous oxide, N_2O, and fluoroacetylene, HCCF. The structural parameters of these and some other related molecules collected in Table I are introduced here for later reference. In this connection, we may also notice that the Lewis structures H–N=C=O and H–O–C≡N are easy to write for isocyanic acid and cyanic acid, respectively. Intuitive Lewis representations for fulminic acid and isofulminic acid, are, however, less obvious due to resonances between single and multiple bond structures.

IV. ELECTRIC PROPERTIES

The electric properties of the four most stable CHNO isomers are summarized in Table II along with available experimental data,[11–19] including the recent results for HOCN (Ref. 18) and HONC (Ref. 19). The dipole moment components μ_i, molecular quadrupole moment tensor Θ_{ij}, and nuclear quadrupole coupling tensors $\chi_{ij}(^{14}N)$, $\chi_{ij}(D)$, and $\chi_{ij}(^{17}O)$ were determined by means of the all electron CCSD(T)/cc-pCV5Z approach at the respective CCSD(T)/cc-pCV5Z(all) equilibrium geometries displayed in Fig. 1.

TABLE I. Structural parameters (in a_0 and degrees) and nuclear quadrupole coupling constants $\chi_{aa}(^{14}N)$ and $\chi_{aa}(D)$ (in MHz) of some molecules related to the CHNO isomer family.

Molecule	Quantity	Value	Ref.
HCN	$r_e(C \equiv N)$	2.186	37
	$r_e(C-H)$	2.008	37
HNC	$r_e(NC)$	2.209	38
	$r_e(HN)$	1.878	38
N_2O	$r_e(NO)$	2.238	39
CO_2	$r_e(C=O)$	2.196	37
HN_3	$r_e(HN)_s$	1.918	40
	$\angle(HNN)_s$	108.8	40
	$\angle(NNN)_s$	171.3	40
HCCF	$r_e(C-H)$	2.004	41
HCN	$\chi_{aa}(^{14}N)$	-4.709	42
	$\chi_{aa}(D)$	0.194	43
HNC	$\chi_{aa}(^{14}N)$	0.264	44
	$\chi_{aa}(D)$	0.262	44
$N_\alpha N_\beta O$	$\chi_{aa}(^{14}N_\alpha)$	-0.774	45
	$\chi_{aa}(^{14}N_\beta)$	-0.268	45
HCCF	$\chi_{aa}(D)$	0.211	46
$HN_\alpha N_\beta N_\gamma$	$\chi_{aa}(^{14}N_\alpha)$	4.85	47
	$\chi_{aa}(^{14}N_\beta)$	-1.35	47

For fulminic acid, the results of the all electron singly augmented CCSD(T)/aug-cc-pCV5Z calculations are additionally shown. Note that the theoretical data in Table II correspond to a vibrationless situation.

The principal axes of the moment-of-inertia tensor are commonly denoted by a, b, c. For the four CHNO isomers, the inertial a axis lies rather close to the nearly linear heavy-atom XYX chain, as readily seen in Fig. 1. There, the angle $\theta(a, \mathbf{r}_{XY})$ between the a axis and the bond distance vector $\mathbf{r}_{XY}$ differs from 0° or 180° by at most 7°.

Takashi et al.[17] reported the dipole moment for several vibrational states of HCNO from CO_2 laser microwave double resonance spectroscopic measurements. The anomalous vibrational dependence of μ was explained by the anharmonic HCN bending potential and studied by means of a simple model, giving an estimate for μ_e of 3.350 ± 0.022 D ($1.318 ea_0$) at the linear configuration. The ground vibrational state value was derived to be $3.099\,345 \pm 0.000\,065$ D ($1.219 ea_0$);[17] to be compared to 3.06 ± 0.15 D obtained from earlier Stark effect measurements.[15] Note that the equilibrium estimate of Takashi et al.[17] is listed for μ_a of HCNO in Table II. The other experimental data correspond, however, to the ground vibrational state.

The microwave and millimeter wave spectroscopic study of HNCO carried out by Hocking et al.[12] gave molecular dipole moment components $|\mu_a|$ and $|\mu_b|$ of $0.620 ea_0$ and $0.531 ea_0$, respectively. Based on electrostatic arguments, supported by several theoretical studies from that time, Hocking et al.[12] concluded that μ_a has a negative sign and μ_b a positive sign in the inertial axis system shown in Fig. 6 of Ref. 12. Since the latter axis system transforms upon $b \rightarrow -b$ into the axis system displayed for HNCO in Fig. 1, the experimental results for μ_a and μ_b of HNCO are both given with a negative sign in Table II, as appropriate for our description of the internal molecular geometry.

The molecular quadrupole moment is given by a traceless second rank tensor Θ, for which $\Theta_{aa} + \Theta_{bb} = -\Theta_{cc}$ holds. For fulminic acid, we also have $\Theta_{bb} = \Theta_{cc} = -\Theta_{aa}/2$ and $\Theta_{ab} = 0$ due to the linear-molecule constraint. As seen in Table II, the constant Θ_{aa} is negative for the nonlinear CHNO isomers. Its positive sign for HCNO is primarily due to a large distance d_H between hydrogen and the molecular center of mass. In Fig. 1, the cc-pCV5Z value for d_H of $4.327 a_0$ for HCNO is to be compared with d_H of 3.713, 3.277, and $3.154 a_0$ for HNCO, HOCN, and HONC, respectively.

The experimental value for Θ_{aa} of HCNO was derived by Hüttner et al.[16] from the susceptibilities estimated in a microwave and rotational Zeeman effect study. This study has also shown that the rotational Zeeman effect in the ground vibrational state of HCNO is adequately described on the basis of a linear-molecule model.

A. Nuclear quadrupole coupling constants

The nuclear quadrupole coupling constant χ_{ij} is the spectroscopic measure of the interaction between the nuclear quadrupole moment Q and the electric field gradient q_{ij}. At the site of a specific nucleus A, the relationship between χ_{ij} and q_{ij} is given by

$$\chi_{ij}(A) = [eQ(A)/h]\, q_{ij}(A), \tag{1}$$

where e is the proton electric charge and h Planck's constant, such that

$$\chi_{ij}(A)[\text{MHz}] = 2.349\,647 Q(A)[\text{fm}^2]\, q_{ij}[E_h/a_0^2]. \tag{2}$$

The electric field gradient tensor q and the nuclear quadrupole coupling tensor χ are both symmetric and traceless, i.e., $\mathcal{D}_{ii} + \mathcal{D}_{jj} + \mathcal{D}_{kk} = 0$ and $\mathcal{D}_{ij} = \mathcal{D}_{ji}$ for $\mathcal{D} = q$ or χ.

In Eqs. (1) and (2), the electric field gradient tensor components q_{ij} are computed first. The theoretically derived nuclear quadrupole coupling constants χ_{ij} are obtained from q_{ij} by multiplication with the known spectroscopic nuclear quadrupole moments. In the case of the CHNO isomer family, the quadrupolar nuclei are $D(I=1)$, $^{14}N(I=1)$, and $^{17}O(I=5/2)$, possessing the nuclear quadrupole moments $Q(D) = 0.286$ fm^2, $Q(^{14}N) = 2.044$ fm^2, and $Q(^{17}O) = -2.558$ fm^2, as given by a "year-2008" compilation due to Pyykkö.[48]

The principal inertial axis tensor is diagonalized to give the eigenvalues $\chi_{\alpha\alpha}$, $\chi_{\beta\beta}$, and $\chi_{\gamma\gamma}$, chosen such that $\chi_{\alpha\alpha}$ is the major principal component of the quadrupole tensor χ and

$$|\chi_{\alpha\alpha}| \geq |\chi_{\beta\beta}| \geq |\chi_{\gamma\gamma}|. \tag{3}$$

For the latter convention, the quadrupole asymmetry parameter η is introduced as

$$\eta = (\chi_{\gamma\gamma} - \chi_{\beta\beta})/\chi_{\alpha\alpha}. \tag{4}$$

Nonzero values of η indicate a deviation from a cylindrical charge distribution around the quadrupole axis α. As seen in Table II, cyanic acid exhibits the highest asymmetry at the

TABLE II. Dipole moments μ_i (in ea_0), quadrupole moments Θ_{ij} (in ea_0^2), and nuclear quadrupole coupling constants $\chi_{ij}(^{14}N)$, $\chi_{ij}(D)$, and $\chi_{ij}(^{17}O)$ (in MHz), computed at the CCSD(T)/cc-pCV5Z level of theory. For HCNO, the CCSD(T)/aug-cc-pCV5Z results are also shown. All calculations have been carried out at the respective CCSD(T)/(aug-)cc-pCV5Z equilibrium geometries. The principal inertial axes are denoted by a, b, c and the principal quadrupole axes by α, β, γ. The angle between the inertial a axis and the quadrupole α axis is abbreviated with $\theta(\alpha,a)$, whereas $\theta(a,\mathbf{r}_{XY})$ stands for the angle between the a axis and the bond distance $\mathbf{r}_{XY}=\mathbf{r}_Y-\mathbf{r}_X$. At the deuterium site, the angle between the α axis and the bond distance $\mathbf{r}_{DX}=\mathbf{r}_D-\mathbf{r}_X$ is $\theta(\alpha,\mathbf{r}_{DX})$. For the definition of the quadrupole asymmetry parameter η, see the main text and Eq. (4). The abbreviations CV5Z and aCV5Z stand for the basis sets cc-pCV5Z and aug-cc-pCV5Z, respectively. The superscript given along with the experimental values indicates the appropriate reference and numbers in parentheses give the uncertainties in units of the last digits.

Property	HNCO CV5Z	HNCO Expt.	HOCN CV5Z	HOCN Expt.	HCNO CV5Z	HCNO aCV5Z	HCNO Expt.	HONC CV5Z	HONC Expt.
μ_a	−0.606	−0.620[a]	−1.370		1.314	1.323	1.318(9)[f]	−1.229	
μ_b	−0.546	−0.531[a]	−0.613					−0.607	
Θ_{aa}	−0.513		−2.025		2.447	2.450	2.2(2)[g]	−2.203	
Θ_{bb}	0.935		2.099		−1.223	−1.225		2.217	
Θ_{ab}	3.047		3.271					3.079	
$\chi_{aa}(^{14}N)$	2.114	2.0527(10)[b]	−2.872	−2.9133(37)[e]	0.294	0.296	0.245(5)[g]	3.225	3.267(4)[i]
$\chi_{bb}(^{14}N)$	−0.556	−0.473(7)[a]	2.076		−0.147	−0.148		−1.854	
$\chi_{ab}(^{14}N)$	1.080		0.104					−0.473	
$\chi_{cc}(^{14}N)$	−1.559	−1.583(7)[a]	0.795		−0.147	−0.148		−1.371	
$\chi_{\alpha\alpha}(^{14}N)$	2.496		−2.874					3.268	
$\chi_{\beta\beta}(^{14}N)$	−1.559		2.079					−1.897	
$\chi_{\gamma\gamma}(^{14}N)$	−0.938		0.795					−1.371	
$\theta(\alpha,a)$	160.5		1.2		0.0	0.0		174.7	
$\theta(a,\mathbf{r}_{XY})$	5.6		3.1		180.0	180.0		4.9	
$\eta(^{14}N)$	0.249		0.447		0.0	0.0		0.161	
$\chi_{aa}(D)$	0.050	0.0565(54)[c]	−0.050	−0.050(12)[e]	0.225	0.225	0.190(25)[g]	−0.057	−0.063(8)[i]
$\chi_{bb}(D)$	0.092		0.217		−0.112	−0.112		0.229	
$\chi_{ab}(D)$	0.204		0.164					0.141	
$\chi_{cc}(D)$	−0.142		−0.167		−0.112	−0.112		−0.172	
$\chi_{\alpha\alpha}(D)$	0.276		0.295					0.287	
$\chi_{\beta\beta}(D)$	−0.142		−0.167					−0.172	
$\chi_{\gamma\gamma}(D)$	−0.134		−0.128					−0.115	
$\theta(\alpha,a)$	48.0	46.9(7)[c]	64.6		0.0	0.0		67.7	
$\theta(a,\mathbf{r}_{XY})$	7.1		4.5		0.0			6.3	
$\theta(\alpha,\mathbf{r}_{DX})$	177.0		177.3		0.0			177.4	
$\eta(D)$	0.031		0.132		0.0	0.0		0.201	
$\chi_{aa}(^{17}O)$	−3.210	−3.276(24)[d]	−8.374		−13.027	−13.019	−12.31(12)[h]	−14.515	
$\chi_{bb}(^{17}O)$	−0.180	−0.176(13)[d]	−1.427		6.514	6.509		0.388	
$\chi_{ab}(^{17}O)$	−0.328		−3.772					−2.440	
$\chi_{cc}(^{17}O)$	3.391	3.452(27)[d]	9.801		6.514	6.509		14.127	
$\chi_{\alpha\alpha}(^{17}O)$	3.391		−10.028					−14.905	
$\chi_{\beta\beta}(^{17}O)$	−3.245		9.801					14.127	
$\chi_{\gamma\gamma}(^{17}O)$	−0.145		0.227					0.777	
$\theta(\alpha,a)$	173.9		156.3		0.0	0.0		170.9	
$\theta(a,\mathbf{r}_{XY})$	5.6		3.0		180.0			4.8	
$\eta(^{17}O)$	0.914		0.955		0.0	0.0		0.896	

[a]Reference 12.
[b]Reference 11.
[c]Reference 13.
[d]Reference 14.
[e]Reference 18.

[f]Reference 17.
[g]Reference 16.
[h]Reference 15.
[i]Reference 19.

site of both ^{14}N and ^{17}O and isofulminic acid at the site of deuterium. Especially large η values are to be noticed at the site of the ^{17}O nucleus for the three nonlinear CHNO members.

The position of the principal quadrupole axes with respect to the inertial axis frame is shown in Fig. 1 for the case of the nitrogen quadrupole tensor $\chi(^{14}N)$. Since the CHNO isomers are planar, such that $\chi_{ci}=0$ for $i=a,b$, the quadru-

pole axis perpendicular to the molecular $a\wedge b$ plane is easy to identify in Table II for the axis convention of Eq. (3). For ^{14}N, the γ axis is parallel to the c axis for HOCN, HCNO, and HONC, whereas the β axis is the quadrupole out-of-plane direction for HNCO, see Fig. 1 and Table II. At the site of deuterium, we additionally see that the deuterium quadrupole tensor is almost aligned with the direction of the bond distance D-X vector $\mathbf{r}_{DX}$. Note also that Heineking et al.[13]
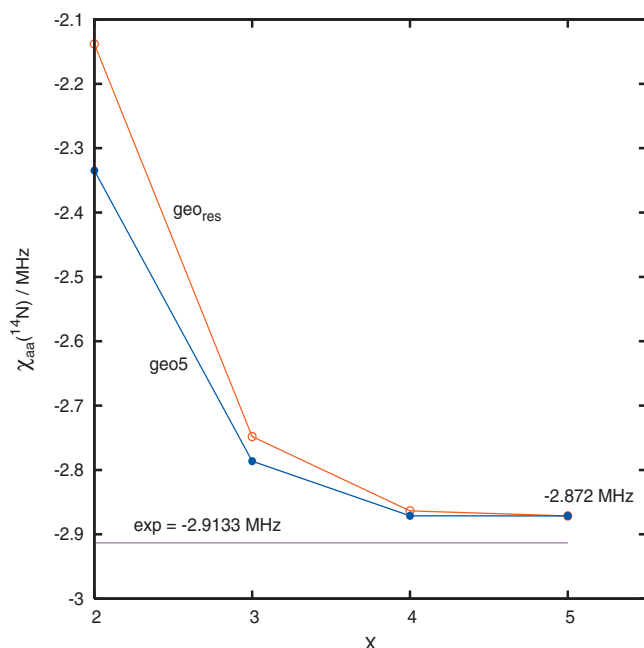
FIG. 2. Variation of the nuclear quadrupole coupling constant $\chi_{aa}(^{14}\text{N})$ of cyanic acid, HOCN, with the basis set cardinal number X of the base cc-pCVXZ. The calculations are carried out at the basis set optimum geometries (geo$_{res}$) and at the quintuple optimum geometry (geo5). The experimental finding (Ref. 18) for $\chi_{aa}(^{14}\text{N})$ is indicated by the horizontal line.

estimated the angle $\theta(\alpha, a)$ between the axes α and a as $46.9 \pm 0.7°$ for DNCO, which agrees nicely with our value of $48°$ in Table II.

The theoretical nuclear quadrupole coupling constants in Table II agree quite well with the few available experimentally derived values. Agreement within approximately 60 kHz is seen for the results at the site of ^{14}N. While the theoretical and experimental data for $\chi_{aa}(\text{D})$ agree within 6 kHz for the nonlinear CDNO isomers, we see a deviation of approximately 35 kHz for DCNO. Note, however, a comparatively large experimental error of 25 kHz for $\chi_{aa}(\text{D})$ of HCNO. In the case of ^{17}O, the agreement is within 60 kHz for HNCO and 0.7 MHz for HCNO. In the CHNO family, vibrational averaging is expected to play a more important role for HCNO and HNCO due to a large amplitude bending motion involving hydrogen.[5,40]

In Fig. 2, we show the variation of the nitrogen nuclear quadrupole coupling constant, $\chi_{aa}(^{14}\text{N})$, of HOCN with the basis set cardinal number X. The upper curve is computed at the geometries geo$_{res}$ optimized separately for each of the cc-pCVXZ basis set members. The second series of calculations, shown by the lower curve, is carried out for X=2–5 at the optimum quintuple geometry geo5. The structural parameters employed were optimized previously.[4,5] As seen in Fig. 2, $\chi_{ij}(^{14}\text{N})$ decreases monotonically upon increasing X, assuming a value of -2.872 MHz at the quintuple level. The cc-pCVQZ/geo$_{res}$ result of -2.864 MHz deviates, thus, by 7 kHz from the corresponding quintuple value, whereas we found a difference of only 0.2 kHz between the cc-pCVQZ/geo5 and cc-pCV5Z/geo5 results.

Similar basis set convergence tests were also carried out for the other three members of the CHNO family. For HNCO, HCNO, and HONC, the quadrupole constants $\chi_{aa}(^{14}\text{N})$ obtained by means of the cc-pCVQZ/geo5 and cc-pCV5Z/geo5 calculations differ, however, by 10, 13, and 23 kHz, respectively. In contrast, the singly augmented aug-cc-pCVQZ/geo5 and aug-cc-pCV5Z/geo5 values for fulminic acid agree within 2 kHz.

Inspection of Table II shows a large negative $\chi_{aa}(^{14}\text{N})$ only for HOCN, which is the only among the four CHNO isomers possessing a triply bound terminal N atom. In addition, HOCN has a positive $\chi_{cc}(^{14}\text{N})$, opposite to HNCO, HCNO, and HONC, for which $\chi_{cc}(^{14}\text{N})$ is negative. The quadrupole constant $\chi_{aa}(^{14}\text{N})$ of HCNO is approximately one order of magnitude smaller than $\chi_{aa}(^{14}\text{N})$ for the nonlinear HNCO, HOCN, and HONC species. The deuterium quadrupole coupling constant $\chi_{aa}(\text{D})$ is positive for HNCO and HCNO, whereas it assumes a negative value for HOCN and HONC. Note that $\chi_{aa}(\text{D})$ of HCNO is the largest among all $\chi_{aa}(\text{D})$ in Table II. The nuclear quadrupole constants $\chi_{aa}(^{17}\text{O})$ at the oxygen site are all large and negative.

Different molecules, possessing a similar electronic environment around a nucleus in question, will have similar nuclear quadrupole coupling constants. The quadrupole constants $\chi_{aa}(^{14}\text{N})$ and $\chi_{aa}(\text{D})$ of several molecules related to the CHNO isomer family are listed in Table I. There, for instance, a large negative $\chi_{aa}(^{14}\text{N})$ value of -4.709 MHz is seen for HCN, whereas nitrogen bound to hydrogen in HN$_3$ is attributed a large positive $\chi_{aa}(^{14}\text{N})$ value of 4.85 MHz. These data may be compared to the nitrogen quadrupole constants of -2.872 MHz for HOCN and 2.114 MHz for HNCO. The constant $\chi_{aa}(^{14}\text{N})$ of 0.264 MHz for HNC is comparable with $\chi_{aa}(^{14}\text{N})$ of 0.294 MHz for HCNO, but much smaller than $\chi_{aa}(^{14}\text{N})$ of 3.225 MHz for HONC. In addition, the deuterium quadrupole constant of 0.225 MHz obtained here for DCNO differs by $+31$, -37, and $+14$ kHz from the $\chi_{aa}(\text{D})$ value for DCN (0.194 MHz), DNC (0.262 MHz), and DCCF (0.211 MHz), respectively. One may note that Hüttner et al.[16] making use of the semiempirical interpretative theory of Townes and Dailey[49,50] have shown in simple terms that the nitrogen quadrupole coupling constant becomes negative in the presence of a lone electron pair and assumes a positive value after removing the lone pair population. For some related results on the electronic structure properties of the CHNO family, see Sec. VI.

The nuclear quadrupole coupling constants $\chi_{ij}(^{14}\text{N})$, $\chi_{ij}(\text{D})$, and $\chi_{ij}(^{17}\text{O})$ reported in Table II are computed for $^{12}\text{CH}^{14}\text{N}^{16}\text{O}$, $^{12}\text{CD}^{14}\text{N}^{16}\text{O}$, and $^{12}\text{CH}^{14}\text{N}^{17}\text{O}$, respectively. Their values for other isotopic species differ from those given in Table II only due to the change in the inertial axis system upon isotopic substitution. For instance, the CDNO inertial axis frame is related to the CHNO frame by a small rotation of approximately 1.5°, giving nitrogen quadrupole constants $\chi_{aa}(^{14}\text{N})$ of 2.169, -2.863, and 3.197 MHz for DNCO, DOCN, and DONC, respectively. These results differ from the respective $\chi_{aa}(^{14}\text{N})$ values of HNCO, HOCN, and HONC in Table II by $\Delta\chi_{aa}^{\text{iso}}$ of $+55$, $+9$, and -28 KHz, where

$$\Delta\chi_{aa}^{\text{iso}} = \chi_{aa}(\text{CDNO}) - \chi_{aa}(\text{CHNO}). \qquad (5)$$

The theoretical differences $\Delta\chi_{aa}^{\text{iso}}$ for nitrogen compare nicely with the experimental values $\Delta\chi_{aa}^{\text{iso}}$ of $+54$, $+7$, and -29 kHz,

derived from the experimental CHNO and CDNO findings for HNCO,[12] HOCN,[18] and HONC,[19] respectively.

The inertial axis system of linear HCNO is not affected by deuterium substitution, such that $\chi_{aa}(^{14}N)$ assumes the same value of 0.294 MHz in HCNO and DCNO.

V. MAGNETIC PROPERTIES

The magnetic dipole moment of a nonzero spin nucleus interacts with the magnetic field generated by the overall molecular rotation, causing thus additional splittings in the rotational spectra. This interaction is described by the so-called nuclear spin-rotation constants C_{ij}. The nuclear contribution to C_{ij} is determined by the molecular geometry only, whereas its electronic contribution is given by the second derivative of the electronic energy with respect to nuclear spin I and rotational angular momentum J.[1] The nuclear magnetic shielding tensor σ, describing the interaction arising from an external magnetic field $\mathcal{B}$, is defined by the second derivative of the electronic energy with respect to the nuclear magnetic moment m and $\mathcal{B}$.[1] The tensor σ is commonly summarized in terms of the isotropic nuclear magnetic shielding σ_{iso}, defined by $\sigma_{iso} = (\sigma_{aa} + \sigma_{bb} + \sigma_{cc})/3$, and the shielding anisotropy $\Delta\sigma$, introduced as $\Delta\sigma = \sigma_{11} - (\sigma_{22} + \sigma_{33})/2$ for $\sigma_{11} \geq \sigma_{22} \geq \sigma_{33}$.

The nuclear spin-rotation constants form a second rank tensor, characterized by $C_{ij} \neq C_{ji}$ for $i \neq j$, where i, j refer to the principal inertial axes a, b, c. For the nonlinear CHNO species, lying in the molecular $a \wedge b$ plane, $C_{ic} = 0$ also holds when $i = a, b$. For HCNO, as common for linear molecules, the tensor C is diagonal with $C_{bb} = C_{cc}$ and $C_{aa} = 0$, where a is the symmetry axis, as seen in Fig. 1.

The magnetic properties calculated in the present work are collected in Table III. There we show the nuclear magnetic shieldings σ_{iso} and anisotropies $\Delta\sigma$, as well as the total nuclear spin-rotation tensor C for each of the four CHNO isomers. The results of Table III were obtained by all electron CCSD(T) correlation calculations, carried out at the respective (aug-)cc-pCV5Z optimum geometries using the basis sets cc-pCVQZ and cc-pCVTZ. The values obtained with the help of the aug-cc-pCVQZ and aug-cc-pCVTZ bases are also shown for the fulminic acid molecule. Among the four [C,H,N,O] atoms of the parent $^{12}CH^{14}N^{16}O$ molecules, only hydrogen and nitrogen possess nonzero magnetic moments m, with $m(H) = +2.792\,847\mu_N$ and $m(^{14}N) = +0.403\,761\mu_N$ where μ_N is the nuclear magneton.[51] In addition to $^{12}CH^{14}N^{16}O$ used to compute the spin-rotation tensors for nitrogen and hydrogen, in Table III we also summarize the spin-rotation tensors at the carbon site and at the oxygen site, determined for $^{13}CH^{14}N^{16}O$ and $^{12}CH^{14}N^{17}O$, respectively. Here, $m(^{13}C) = +0.702\,412\mu_N$ and $m(^{17}O) = -1.893\,80\mu_N$.[51]

Comparison of the triple and quadruple ζ results of Table III shows convergence within 5 ppm for σ_{iso} and $\Delta\sigma$. The components of the spin-rotation tensor are converged within 0.09 kHz for the nitrogen center, 2 kHz for hydrogen, 0.33 kHz for carbon, and 0.56 kHz for oxygen.

In Table III, HNCO at the nitrogen site, HOCN at the carbon site, and HONC at the nitrogen and hydrogen sites

have one diagonal spin-rotation constant C_{ii} differing in sign from the other two. Under these circumstances, the rotational magnetic field may vanish for certain orientations, giving rise to a logarithmic singularity in the resonance shape.[52] Note also that the magnitude of the spin-rotation components $C_{aa}(H)$ and $C_{ab}(H)$ of the nonlinear CHNO isomers are noticeably larger than all other contributions. In molecular systems containing quadrupolar ^{14}N and magnetic H, like in the case of HNCO, terms involving hydrogen spin are not (well) resolved due to the much stronger nitrogen quadrupole interactions.[11]

From splittings of the rotational state 1_{01} in molecular beam microwave spectra of isocyanic acid, Kukolich et al.[11] derived nitrogen spin-rotation interaction strength constants $C_N(1_{01})$ of 0.50 ± 0.2 kHz and 0.55 ± 0.2 kHz for HNCO and DNCO, respectively, and the deuterium $C_D(1_{01})$ value of 0.76 ± 0.1 kHz. Since DNCO possesses two quadrupolar nuclei, the interaction parameters of DNCO were obtained by a two-step procedure using the appropriate coupling scheme.[11]

For a given rotational state $J_{K_a K_b}$, the spin-rotation interaction strength constant $C(J_{K_a K_b})$ is related to the spin-rotation tensor components C_{ij} after rotational averaging by the expression[53,54]

$$C(J_{K_a K_b}) = \sum_{q=a,b,c} C_{qq}\langle J_q^2\rangle/J(J+1), \tag{6}$$

where $\langle J_q^2\rangle$ is the average value of the square of the rotational angular momentum component J_q in the direction of the inertial axis $q = a, b, c$. For a prolate top with the symmetry axis along a, it follows

$$\langle J_a^2\rangle = K_a^2,$$

$$\langle J_b^2\rangle = \langle J_c^2\rangle = [J(J+1) - K_a^2]/2, \tag{7}$$

such that

$$C(1_{01}) = (C_{bb} + C_{cc})/2 = C_\perp \tag{8}$$

for the rotational state 1_{01}. Since HNCO is a nearly prolate symmetric top ($\kappa \approx -1$), use of Eq. (8) yields the theoretical estimate for $C(1_{01})$ of 0.62 kHz for nitrogen and of -0.79 kHz for hydrogen, see Table III. Additional CCSD(T) calculations carried out for DNCO have revealed $C_N(1_{01})$ of 0.58 kHz and $C_D(1_{01})$ of -0.11 kHz for this species. As seen, the theoretical values for $C_N(1_{01})$ of HNCO and DNCO are in excellent agreement with the experimental findings of Kukolich et al.[11] However, the experimental and theoretical results for the deuterium $C_D(1_{01})$ constant differ and are of different signs.

It is worthy noting that the HNCO and DNCO results for the spin-rotation strengths are related by

TABLE III. Nuclear magnetic shieldings σ_{iso} (in ppm), nuclear magnetic anisotropies $\Delta\sigma$ (in ppm), and total spin-rotation tensor components C_{ij} (in kHz) from the all electron CCSD(T) calculations at the respective CCSD(T)/(aug-)cc-pCV5Z optimum geometries. The basis sets cc-pCVXZ and aug-cc-pCVXZ are abbreviated with, respectively, CVXZ and aCVXZ for X=T and Q. The parameter $\bar{C}$ stands for $(C_{aa}+C_{bb}+C_{cc})/3$ and $C_\perp$ for $(C_{bb}+C_{cc})/2$.

Atomic center ^{14}N	HNCO		HOCN		HCNO			HONC	
	CVQZ	CVTZ	CVQZ	CVTZ	CVQZ	aCVQZ	aCVTZ	CVQZ	CVTZ
σ_{iso}	242	243	94	96	60	60	63	94	97
$\Delta\sigma$	158	156	354	350	439	439	434	391	387
C_{aa}	−1.54	−1.57	3.85	3.86				−0.69	−0.67
C_{bb}	0.77	0.76	1.47	1.46	2.00	2.00	1.97	1.74	1.72
C_{cc}	0.47	0.46	1.69	1.68	2.00	2.00	1.97	1.62	1.60
C_{ba}	0.18	0.18	0.00	0.00				−0.13	−0.13
C_{ab}	−12.14	−12.05	0.57	0.63				0.69	0.61
$\bar{C}$	−0.10	−0.11	2.34	2.33	1.33	1.33	1.31	0.89	0.88
$C_\perp$	0.62	0.61	1.58	1.57	2.00	2.00	1.97	1.68	1.66

Atomic center H	HNCO		HOCN		HCNO			HONC	
	CVQZ	CVTZ	CVQZ	CVTZ	CVQZ	aCVQZ	aCVTZ	CVQZ	CVTZ
σ_{iso}	29	29	28	28	29	29	29	26	26
$\Delta\sigma$	18	18	20	20	17	17	17	16	16
C_{aa}	−56.01	−57.19	−64.36	−66.20				−63.88	−65.56
C_{bb}	−0.27	−0.28	−0.06	−0.07	−1.24	−1.25	−1.26	0.38	0.37
C_{cc}	−1.30	−1.32	−1.22	−1.25	−1.24	−1.25	−1.26	−1.23	−1.26
C_{ba}	0.88	0.88	0.58	0.59				0.69	0.69
C_{ab}	45.21	46.10	31.22	32.01				26.16	26.84
$\bar{C}$	−19.20	−19.60	−21.88	−22.50	−0.83	−0.83	−0.84	−21.58	−22.15
$C_\perp$	−0.79	−0.80	−0.64	−0.66	−1.24	−1.25	−1.26	−0.43	−0.45

Atomic center ^{13}C	HNCO		HOCN		HCNO		HONC	
	CVQZ	CVTZ	CVQZ	CVTZ	aCVQZ	aCVTZ	CVQZ	CVTZ
σ_{iso}	55	59	81	84	173	175	79	82
$\Delta\sigma$	323	319	309	304	164	161	287	283
C_{aa}	21.00	20.67	−1.19	−1.02			6.31	6.26
C_{bb}	4.99	4.90	4.43	4.36	2.26	2.20	4.29	4.22
C_{cc}	5.11	5.02	4.25	4.18	2.26	2.20	4.50	4.42
C_{ba}	−0.72	−0.71	−0.05	−0.05			0.08	0.07
C_{ab}	−0.01	−0.01	1.44	1.34			−7.25	−7.01
$\bar{C}$	10.37	10.20	2.50	2.50	1.51	1.47	5.03	4.96
$C_\perp$	5.05	4.96	4.34	4.27	2.26	2.20	4.40	4.32

Atomic center ^{17}O	HNCO		HOCN		HCNO		HONC	
	CVQZ	CVTZ	CVQZ	CVTZ	aCVQZ	aCVTZ	CVQZ	CVTZ
σ_{iso}	194	195	308	309	222	222	217	218
$\Delta\sigma$	266	264	99	98	296	293	215	215
C_{aa}	−32.98	−33.28	−21.30	−20.91			−25.56	−25.48
C_{bb}	−2.00	−1.98	−1.01	−1.00	−2.44	−2.40	−2.47	−2.47
C_{cc}	−2.95	−2.93	−0.87	−0.85	−2.44	−2.40	−1.80	−1.78
C_{ba}	0.42	0.44	0.01	0.01			−0.01	0.00
C_{ab}	3.64	3.46	14.19	13.87			12.52	11.96
$\bar{C}$	−12.64	−12.73	−7.73	−7.59	−1.62	−1.60	−9.94	−9.91
$C_\perp$	−2.47	−2.45	−0.94	−0.93	−2.44	−2.40	−2.13	−2.12

$$C_{\text{N}}^{\text{DNCO}} = (B_{\text{eff}}^{\text{DNCO}}/B_{\text{eff}}^{\text{HNCO}})C_{\text{N}}^{\text{HNCO}},$$

$$C_{\text{D}}^{\text{DNCO}} = (B_{\text{eff}}^{\text{DNCO}}/B_{\text{eff}}^{\text{HNCO}})(\gamma_{\text{D}}/\gamma_{\text{H}})C_{\text{H}}^{\text{HNCO}}, \qquad (9)$$

where B_{eff} stands for the average value $(B+C)/2$, whereas γ_{H} and γ_{D} are the magnetogyric ratios for hydrogen

and deuterium, i.e., $\gamma_{\text{H}} = 2m(\text{H})$ and $\gamma_{\text{D}} = m(\text{D})$, using $m(\text{D}) = 0.857\,438\,2\mu_N$. The effective constants B_{eff} computed from the CCSD(T)/cc-pCV5Z optimum geometry of Fig. 1 are 11 038 and 10 240 MHz for HNCO and DNCO, respectively. Equation (9) provides an independent check of the

accuracy of the derived spectroscopic parameters and can be used to estimate the parameter values for other isotopic species from the data collected in Table III.

For comparative purposes, we additionally give our CCSD(T)/aug-cc-pCVQZ results for the nuclear spin-rotation coupling constants (C_H, C_N) of hydrogen cyanide and hydrogen isocyanide, obtained to be $(-4.71, 9.91 \text{ kHz})$ for HCN and $(-4.69, 6.55 \text{ kHz})$ for HNC. A comparison of the latter results with the $C_\perp$ values for the CHNO family in Table III shows that the hydrogen constants assume negative values and the nitrogen constants positive values for both HNC/HCN and CHNO systems. Their absolute values are different due to different rotational constants among other effects.

Regarding HCN/HNC, the experimentally derived ground vibrational state values for (C_H, C_N) are $(-4.35 \pm 0.05 \text{ kHz}, 10.13 \pm 0.02 \text{ kHz})$ for HCN (Ref. 55) and C_N of 7.15 ± 1.09 kHz for HNC.[44] More recent results of Bechtel *et al.*[56] for C_N given as 9.99 ± 0.43 kHz for HCN and as 6.79 ± 0.10 kHz for HNC are in even better agreement with our findings. We may also note that our all electron CCSD(T)/aug-cc-pCVQZ equilibrium parameters, given by $r_e(\text{HC}) = 2.0140 a_0$ and $r_e(\text{CN}) = 2.1810 a_0$ for HCN and by $r_e(\text{HN}) = 1.8815 a_0$ and $r_e(\text{NC}) = 2.2102 a_0$ for HNC, are in excellent agreement with the earlier theoretical results.[57]

VI. ELECTRONIC STRUCTURE PROPERTIES

The CHNO isomers possess planar equilibrium geometries of *trans* type.[5] For nonlinear HNCO, HOCN, and HONC in C_s symmetry, the reference (self-consistent field) electronic configuration is given by

$$(\text{core})^6 (4a')^2 (5a')^2 (6a')^2 (7a')^2 (1a'')^2 (8a')^2 (9a')^2 (2a'')^2,$$

where the core contribution $(1a')^2 (2a')^2 (3a')^2$ stands for the three $1s$-like core orbitals located on oxygen, nitrogen, and carbon, respectively. The linear HCNO molecule, described by

$$(\text{core})^6 (4\sigma^+)^2 (5\sigma^+)^2 (6\sigma^+)^2 (7\sigma^+)^2 (1\pi)^4 (2\pi)^4,$$

possesses two pairs, $(1\pi_x, 1\pi_y)$ and $(2\pi_x, 2\pi_y)$, of degenerate π orbitals.

The molecular orbitals of nonlinear HNCO, HOCN, and HONC are displayed in Fig. 3, whereas the molecular orbitals of linear HCNO are found in Fig. 4. The highest occupied molecular $2a''$ orbitals (HOMOs) of HNCO, HOCN, and HONC and the orbital pair $(2\pi_x, 2\pi_y)$ of HCNO are composed essentially from the out-of-plane $2p_x$ orbitals (as well as $2p_y$ in the case of linear HCNO) located on O, C, and N. The orbital contribution associated with oxygen in the HOMOs can be interpreted as a lone electron pair in all four cases.

The molecular orbitals depicted in Figs. 3 and 4 for the four CHNO isomers are of similar shape, although with somewhat different order on the energy scale. The latter affects solely the molecular orbitals designated as $7a'$, $8a'$, $9a'$ in C_s symmetry. We see that the molecular orbitals $(8a', 7a', 9a')$ of HOCN and $(9a', 8a', 7a')$ of

HONC readily correlate with $(7a', 8a', 9a')$ of HNCO. The orbitals $7\sigma^+$ and $(1\pi_x, 1\pi_y)$ of HCNO correlate with respectively $9a'$ and $(7a', 8a')$ of HONC. In other words, hydrogen migration from HNCO to HOCN and hydrogen migration from HCNO to HONC is followed by reversal of the position of one σ-like and one π-like orbital, such that the σ-type orbital lies above the π-type orbital in the more energetic HOCN and HONC. A similar effect of molecular orbital $\sigma - \pi$ reordering occurs also in HCN$\rightarrow$HNC, as seen in Fig. 5. The orbital $5\sigma^+$ is energetically below the $(1\pi_x, 1\pi_y)$ orbital pair in the case of HCN, whereas the opposite situation with $5\sigma^+$ being above $(1\pi_x, 1\pi_y)$ characterizes HNC. Note that Figs. 3–5 of the present work were drawn with the help of the pre- and postprocessing program MOLDEN.[58]

The common feature of the molecular σ-like orbitals $7a'$ of HNCO, $8a'$ of HOCN, $7\sigma^+$ of HCNO, and $9a'$ of HONC in these four HXYZ isomers is the promotion of p_z electrons along the molecular z axis toward the terminal atom Z, resulting in a prominent electron cloud on Z, as seen in Figs. 3 and 4. The same is also true for the molecular orbitals $5\sigma^+$ of HCN and HNC in Fig. 5. In view of this, we may expect larger dipole moments for the more energetic HOCN and HONC species than for HNCO and HCNO, as verified with the help of Table II, yielding $|\mu|(\text{HNCO}) = 0.816 e a_0$ versus $|\mu|(\text{HOCN}) = 1.501 e a_0$ and $|\mu|(\text{HCNO}) = 1.314 e a_0$ versus $|\mu|(\text{HONC}) = 1.371 e a_0$ from the CCSD(T)/cc-pCV5Z data. The difference between the two $|\mu|$ values smaller for the HCNO/HONC isomer pair than for HNCO/HOCN may readily be related to a smaller σ-π energy separation in HCNO/HONC than in HNCO/HOCN. Further confirmation of this qualitative picture is provided also by HCN/HNC, where the dipole moment of $1.224 e a_0$ for HNC is to be compared with $\mu_e(\text{HCN})$ of $1.187 e a_0$ at the CCSD(T)/aug-cc-pCVQZ level of calculation.

Spherically symmetric closed shells produce zero average field at the nucleus and hence do not contribute to the electric field gradient.[49] Nonzero electric field gradients, i.e., nuclear quadrupole interactions, are primarily due to nonspherical charge distributions among the p_x, p_y, and p_z orbitals, as put forward by Townes and Dailey.[49,50] To gain further insight into the electron subspace of the CHNO family in simple terms, the results of the Mulliken population analysis[59] of the total CCSD(T)/cc-pCV5Z density by the individual basis function (orbital) type are summarized in Table IV. The corresponding results obtained for HCN and HNC from the total CCSD(T)/aug-cc-pCVQZ electron density are collected in Table V. In these two tables, p_z and p_y stand for the in-plane p orbitals and p_x for the normal-to-the-plane functions. Note that the Mulliken population analysis is used here only for qualitative purposes. Other electronic population analyses, such as a natural bond orbital (NBO) approach[60] or atoms-in-molecules (AIM) approach,[61] may provide somewhat different electron populations.

Along the H-X-Y-Z chain in Table IV, the partial (Mulliken) charges on the four atomic [C,H,N,O] centers are alternating between positive and negative, leading systematically to the structure +HXYZ−. Oxygen is negatively charged in all four CHNO isomers, as expected for the most electronegative among the four [C,H,N,O] elements. Nitro-
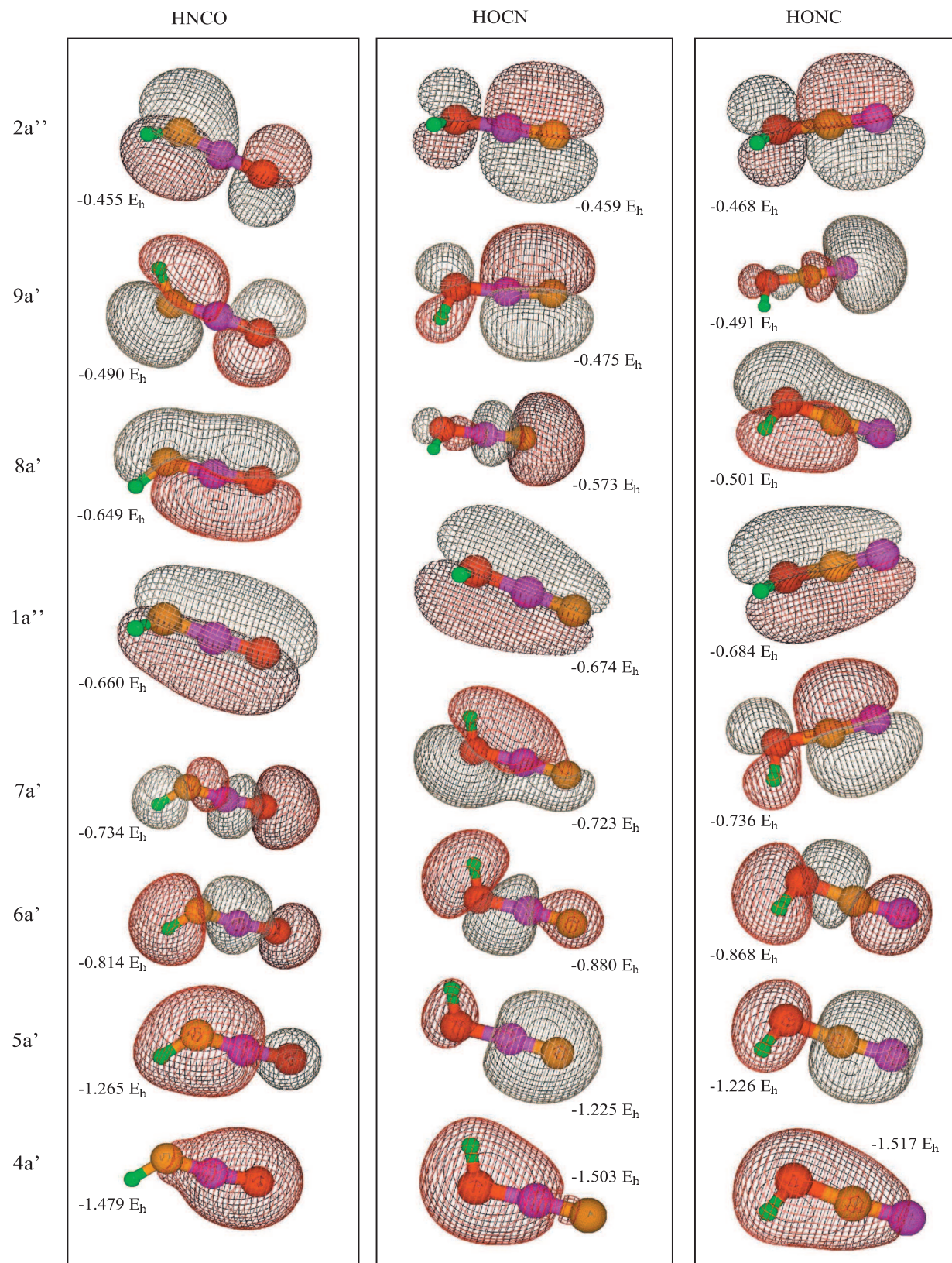
FIG. 3. Molecular orbitals of HNCO, HOCN, and HONC. The contour surfaces of the orbital amplitude 0.025 are shown. The orbital energies are taken from the cc-pCV5Z calculations.

gen is negatively charged and carbon positively in HNCO and HOCN (see Table IV), as expected on account of the higher electronegativity of N relative to C. Carbon is somewhat more positively charged in HOCN than in HNCO, since C is involved in a triple bond in HOCN. In HCNO and HONC, the situation is opposite and characterized by positively charged nitrogen and negatively charged carbon. This may qualitatively be interpreted as due to a lone electron pair of nitrogen, participating in binding with carbon through an orbital of σ-type symmetry.
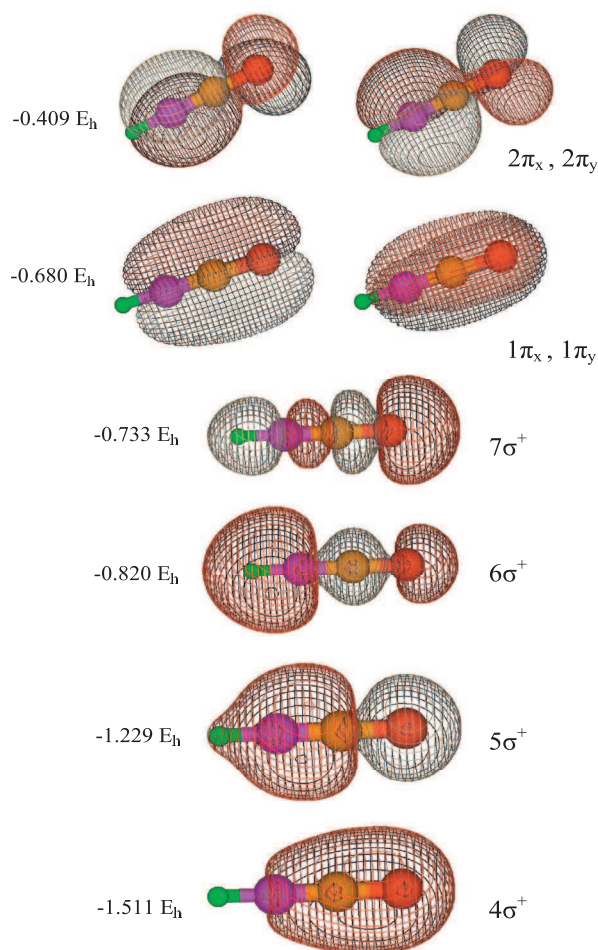
FIG. 4. Same as Fig. 3, only for the HCNO molecule.

Chemical binding involves mixing of valence electrons. While a defect of p_z electrons is an indication of π-type binding, an excess of p_z electrons is typical for hybrid bonds involving s and p_z orbitals.[50] These effects are considered first for HCN/HNC for the purpose of illustration. In Table V, the p_z character on N increases for HCN and decreases for

HNC with respect to the free atom situation. We also see that the p_z population on N is larger for HCN and smaller for HNC than the respective $p_y = p_x$ contribution. Different electronic environments around nitrogen in these two molecules result in different electric field gradient tensors. To be specific, electric field gradient components $q_{aa}(N)$ of -0.967 E_h/a_0^2 for HCN and 0.066 E_h/a_0^2 for HNC were obtained in the aug-cc-pCVQZ calculations, yielding $\chi_{aa}(^{14}N)$ of -4.645 and 0.317 MHz for, respectively, HCN and HNC, in good agreement with the theoretical $\chi_{aa}(^{14}N)$ values of Wong.[62] At the hydrogen site, we obtain $q_{aa}(H)$ of 0.318 and 0.416 E_h/a_0^2 for HCN and HNC, giving thus $\chi_{aa}(D)$ of 0.214 and 0.279 MHz, respectively. The related experimental ground vibrational state values are $\chi_{aa}(^{14}N)$ of $-4.707\,83 \pm 0.000\,06$ MHz (Ref. 55) and $\chi_{aa}(D)$ of 0.1944 ± 0.0022 MHz (Ref. 43) for HCN, and $\chi_{aa}(^{14}N)$ of 0.2641 ± 0.0010 MHz (Ref. 56) and $\chi_{aa}(D)$ of 0.2619 ± 0.0145 MHz (Ref. 44) for HNC.

In Fig. 5, somewhat similar electronic environments may be noticed around the terminal N atom in HCN and the terminal C atom in HNC with, however, different ordering of the $5\sigma^+$ and $(1\pi_x, 1\pi_y)$ orbitals. This is supported by the fact that the electric field gradient component $q_{aa}(N)$ of -0.967 E_h/a_0^2 for N in HCN is comparable with $q_{aa}(C)$ of -0.811 E_h/a_0^2 for C in HNC. This is not the case for the electric field gradients for the central nucleus, as seen from $q_{aa}(C)$ of -0.361 E_h/a_0^2 in HCN and $q_{aa}(N)$ of 0.066 E_h/a_0^2 in HNC. Note also that the CCSD(T)/aug-cc-pCVQZ equilibrium bond length $r_e(CN)$ of $2.210a_0$ in HNC is $0.029a_0$ longer than the triple bond $r_e(C\equiv N)$ distance of $2.181a_0$ in HCN (see Sec. V) and $0.084a_0$ shorter than the double bond $r_e(C=N)$ value of $2.294a_0$ in HNCO (see Fig. 1). In conclusion, we may write $H-N^+\equiv C^-$ as a probable simple valence bond structure of hydrogen isocyanide.

The results of the population analysis for the CHNO isomer family in Table IV exhibit features similar to the HCN/HNC situation. A decrease in the s character with respect to the free atom situation is seen for all nuclear centers, except for C in HONC. Nitrogen and oxygen bear an excess
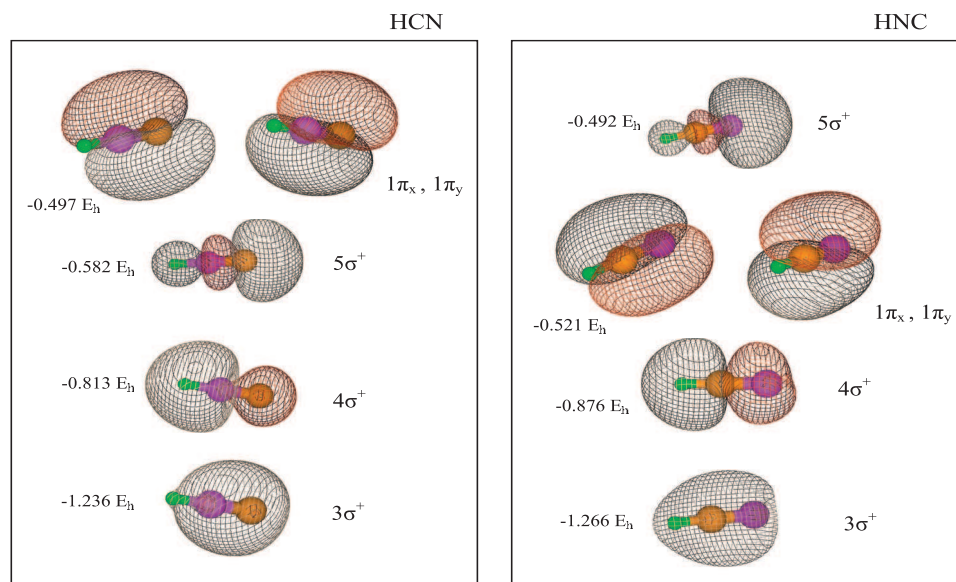

FIG. 5. Molecular orbitals of HCN (left) and HNC (right). The contour surfaces of the orbital amplitude 0.025 are shown. The orbital energies are taken from the aug-cc-pCVQZ calculations.

TABLE IV. Population analysis for the CHNO isomer family of the total CCSD(T)/cc-pCV5Z electron density by basis function (orbital) type.

HNCO	s	p_z	p_y	p_x	Total	Charge
H	0.67	0.03	0.02	0.04	0.77	+0.23
N	3.47	1.13	1.27	1.39	7.37	−0.37
C	2.90	0.80	0.76	0.82	5.61	+0.39
O	3.75	1.37	1.48	1.57	8.25	−0.25
HOCN	s	p_z	p_y	p_x	Total	Charge
H	0.58	0.03	0.02	0.04	0.70	+0.30
O	3.77	1.29	1.44	1.78	8.36	−0.36
C	2.85	0.70	0.91	0.87	5.49	+0.51
N	3.86	1.21	1.08	1.16	7.45	−0.45
HCNO	s	p_z	p_y	p_x	Total	Charge
H	0.78	0.03	0.02	0.02	0.85	+0.15
C	3.06	0.86	1.02	1.02	6.08	−0.08
N	3.22	1.00	1.18	1.18	6.75	+0.25
O	3.79	1.12	1.66	1.66	8.32	−0.32
HONC	s	p_z	p_y	p_x	Total	Charge
H	0.59	0.02	0.02	0.05	0.69	+0.31
O	3.79	1.08	1.45	1.83	8.24	−0.24
N	3.25	0.82	1.35	1.31	6.86	+0.14
C	4.04	0.74	0.61	0.68	6.21	−0.21

of p_x and p_y electrons. An excess of p_z electrons on N is seen for HNCO and HOCN, while a defect of p_z electrons occurs in HONC. This finding can be compared to the HCN and HNC case, respectively. It is also noteworthy that the p_z population on N for HOCN and HCN is the largest among the three p contributions, due to the lone pair electrons (σ-type binding), and that the nuclear quadrupole constants $\chi_{aa}(^{14}N)$ of HOCN and HCN are both large and negative. On the other hand, HNCO, HCNO, HONC, and HNC possess the largest p population different from p_z (π-type binding) and positive $\chi_{aa}(^{14}N)$. At the oxygen site, the largest p population is p_x and the four CHNO isomers have $\chi_{aa}(^{17}O)$ of the same sign, as seen in Table II.

Townes and Dailey[49] explained a large negative quadrupole constant $\chi_{aa}(^{75}As)$ of −235 MHz for AsF$_3$ by an excess of p_z electrons, arising from $s-p$ hybridization in this molecular system with single bonds only. For the CHNO family,

we see that a sign of the nuclear quadrupole constant in the presence of multiple bonds is determined by the largest among the three p contributions. A nice example for this effect is given by the HNCO and HOCN pair. Whereas the two molecules both exhibit an increase of nitrogen p_z electrons with respect to the free atom situation in Table IV, the nitrogen quadrupole constants $\chi_{aa}(^{14}N)$ in Table II are of comparable magnitudes but of different signs, due to different major p components, p_x versus p_z.

The electric field gradients q_{aa} around the terminal atoms of the nonlinear HOCN and HONC molecules are found to be comparable. Namely, we obtained $q_{aa}(N)$ of −0.598 E_h/a_0^2 for HOCN and $q_{aa}(C)$ of −0.578 E_h/a_0^2 for HONC. This finding indicates similar electronic environments, i.e., similar binding mechanisms, for N in HOCN and C in HONC. Since the bond length $r_e(CN)$ of 2.218a_0 in HONC is very close to $r_e(CN)$ of 2.210a_0 in HNC, the geo-

TABLE V. Population analysis for HCN and HNC of the total CCSD(T)/aug-cc-pCVQZ electron density by basis function (orbital) type.

HCN	s	p_z	p_y	p_x	Total	Charge
H	0.47	0.00	0.01	0.01	0.49	+0.52
C	3.34	0.95	0.85	0.85	6.08	−0.08
N	3.85	1.30	1.08	1.08	7.44	−0.44
HNC	s	p_z	p_y	p_x	Total	Charge
H	0.67	0.02	0.03	0.03	0.77	+0.23
N	3.49	0.96	1.31	1.31	7.13	−0.13
C	3.74	1.01	0.60	0.60	6.10	−0.10

metric arguments presented above in connection with HNC can be employed also for HONC. All this shows that we may write $H-O-N^+\equiv C^-$ as a probable dominant valence bond structure of isofulminic acid, in analogy with the HNC case.

A. Fulminic acid

We summarize now some electronic structure and geometric properties derived in the present work for fulminic acid.

At the hydrogen site, the electric field gradients $q_{aa}(H)$ of 0.335 E_h/a_0^2 for HCNO and 0.318 E_h/a_0^2 for HCN are comparable, yielding similar $\chi_{aa}(D)$ values for these two molecules (Table II and Sec. VI). Compared to HNCO, HOCN, and HONC, fulminic acid possesses an enhanced positive deuterium quadrupole constant $\chi_{aa}(D)$.

The bond lengths $r_e(CN)$ and $r_e(HC)$ of HCNO and HCN agree within $0.006a_0$, as seen in Table I and Fig. 1. The electric field gradient $q_{aa}(C)$ found to be -0.005 E_h/a_0^2 in HCNO is, however, noticeably different from $q_{aa}(C)$ of -0.361 E_h/a_0^2 in HCN. A small $q_{aa}(C)$ value indicates a nearly spherically symmetric charge distribution around C in HCNO. In addition, $q_{aa}(C)$ of HCNO differs from both $q_{aa}(N)$ of 0.440 E_h/a_0^2 and $q_{aa}(C)$ of -0.479 E_h/a_0^2 in HNCO. The carbon p_z population in HCNO is larger than the $p_x = p_y$ contributions. Similar properties of the p population are also seen for HOCN, Table II. However, the $q_{aa}(C)$ value of -0.126 E_h/a_0^2 for HOCN is also different from the corresponding HCNO value. Furthermore, the electric field around the carbon center of HCNO is found to be different from all other local nuclear fields.

The nitrogen quadrupole constant of 0.296 MHz for HCNO is compatible with $\chi_{aa}(^{14}N)$ of 0.317 MHz for HNC and of much smaller magnitude than $\chi_{aa}(^{14}N)$ of -4.645 MHz for HCN. The nitrogen p distribution in HCNO compares more favorably with the corresponding results for HNC than HCN.

Oxygen is a common terminal atom of HNCO and HCNO, in addition to H. The respective oxygen quadrupole constants of -3.210 and -13.027 MHz are, however, very different (Table II). In Table IV, oxygen exhibits an excess of p_z electrons for HNCO and a defect for HCNO. Note that $r_e(OC)=2.456a_0$ of HOCN and $r_e(ON)=2.513a_0$ of HONC are 0.18 and $0.24a_0$ longer than $r_e(NO)=2.271a_0$ for HCNO, Fig. 1. The latter distance is $0.016a_0$ longer than the double $N=O$ bond of $2.255a_0$ for NO_2.[39] In addition, HCNO and HONC possess comparable $\chi_{aa}(^{17}O)$ constants, Table II.

VII. CONCLUSION

This paper provides an extensive study of the electric and magnetic properties of isocyanic acid, cyanic acid, fulminic acid, and isofulminic acid, representing the four most stable CHNO isomers. Our analysis covers (a) determination of the dipole moment components, molecular quadrupole moments, and nuclear quadrupole coupling constants at the site of the quadrupolar ^{14}N, D, and ^{17}O nuclei, (b) determination of the nuclear spin-rotation coupling parameters, and

(c) investigation of the electronic structure properties by means of the electric field gradients in conjunction with the results of a Mulliken population analysis.

The properties studied in this work are useful to molecular spectroscopists. In view of very recent laboratory advances in observing the previously spectroscopically unknown HOCN and HONC molecules and very recent identifications of HCNO and HOCN in several interstellar regions, including vibrationally excited HNCO, our results assume some importance for further experimental investigations on these challenging molecular systems.

[1] W. H. Flygare, Chem. Rev. (Washington, D.C.) **74**, 653 (1974).
[2] W. H. Flygare, J. Chem. Phys. **41**, 793 (1964).
[3] C. H. Townes and A. L. Schawlow, *Microwave Spectroscopy* (Dover, New York, 1975).
[4] M. Mladenović and M. Lewerenz, Chem. Phys. **343**, 129 (2008).
[5] M. Mladenović, M. Elhiyani, and M. Lewerenz, J. Chem. Phys. **130**, 154109 (2009).
[6] M. S. Schuurman, S. R. Muir, W. D. Allen, and H. F. Schaefer III, J. Chem. Phys. **120**, 11586 (2004).
[7] Note that the dipole moment components μ_a and μ_b of isocyanic acid, HOCN, are interchanged on page 131 of Ref. 4. The correct RHF/cc-pV5Z dipole moment results are thus $|\mu_a|=3.715$ D and $|\mu_b|=1.642$ D for HOCN.
[8] J. H. Teles, G. Maier, B. A. Hess, Jr., L. J. Schaad, M. Winnewisser, and B. P. Winnewisser, Chem. Ber. **122**, 753 (1989), and references therein.
[9] L. H. Jones, J. N. Shoolery, R. G. Shulman, and D. M. Yost, J. Chem. Phys. **18**, 990 (1950).
[10] A. V. Lapinov, G. Y. Golubiatnikov, V. N. Markov, and A. Guarnieri, Astron. Lett. **33**, 121 (2007).
[11] S. G. Kukolich, A. C. Nelson, and B. S. Yamanashi, J. Am. Chem. Soc. **93**, 6769 (1971).
[12] W. H. Hocking, M. C. L. Gerry, and G. Winnewisser, Can. J. Phys. **53**, 1869 (1975).
[13] N. Heineking, M. C. L. Gerry, and H. Dreizler, Z. Naturforsch. A **44**, 577 (1989).
[14] M. C. L. Gerry, S. J. Howard, N. Heineking, and H. Dreizler, Z. Naturforsch. A **44**, 1187 (1989).
[15] M. Winnewisser and H. K. Bodenseh, Z. Naturforsch. A **22**, 1724 (1967).
[16] W. Hüttner, H. K. Bodenseh, P. Nowicki, and K. Morgenstern, J. Mol. Spectrosc. **71**, 246 (1978).
[17] R. Takashi, K. Tanaka, and T. Tanaka, J. Mol. Spectrosc. **138**, 450 (1989).
[18] S. Brünken, C. A. Gottlieb, M. C. McCarthy, and P. Thaddeus, Astrophys. J. **697**, 880 (2009).
[19] M. C. McCarthy and P. Thaddeus, private communication (22 September 2008).
[20] D. Quan, E. Herbst, and Y. Osamura (unpublished).
[21] D. Buhl, L. E. Snyder, and J. Edrich, Nature (London) **243**, 513 (1973).
[22] N. Q. Rieu, C. Henkel, J. M. Jackson, and R. Mauersberger, Astron. Astrophys. **241**, L33 (1991).
[23] C. Knez, J. H. Lacy, N. J. Evans II, E. F. van Dishoeck, and M. J. Richter, Astrophys. J. **696**, 471 (2009).
[24] N. Marcelino, J. Cernicharo, N. B. Tercero, and E. Roueff, Astrophys. J. **690**, L27 (2009).
[25] S. Brünken, A. Belloche, S. Martín, L. Verheyen, and K. M. Menten, Astron. Astrophys. (submitted).
[26] B. E. Turner, Astrophys. J., Suppl. Ser. **136**, 579 (2001).

[27] S. Huber, Phys. Rev. A **31**, 3981 (1985).

[28] R. Eggenberger, S. Gerber, H. Huber, D. Searles, and M. Welker, J. Mol. Spectrosc. **151**, 474 (1992).

[29] R. Ludwig, F. Weinhold, and T. C. Farrer, J. Chem. Phys. **105**, 8223 (1996).

[30] W. C. Bailey, Chem. Phys. **252**, 57 (2000).

[31] T. H. Dunning, Jr., J. Chem. Phys. **90**, 1007 (1989).

[32] D. E. Woon and T. H. Dunning, Jr., J. Chem. Phys. **103**, 4572 (1995).

[33] ACES2, Mainz-Austin-Budapest version, a package of *ab initio* programs, J. F. Stanton, J. Gauss, J. D. Watts, P. G. Szalay, R. J. Bartlett *et al.* For the current version, see http://www.aces2.de.

[34] J. F. Stanton, J. Gauss, J. D. Watts, W. J. Lauderdale, and R. J. Bartlett, Int. J. Quantum Chem. Symp. **26**, 879 (1992).

[35] J. Gauss and J. F. Stanton, J. Chem. Phys. **104**, 2574 (1996).

[36] J. Gauss, K. Ruud, and T. Helgaker, J. Chem. Phys. **105**, 2804 (1996).

[37] G. Herzberg, *Molecular Spectra and Molecular Structure*, Infrared and Raman Spectra of Polyatomic Molecules Vol. II (corrected reprint of 1945 edition) (Krieger, Malabar, FL, 1991).

[38] R. A. Creswell and A. G. Robiette, Mol. Phys. **36**, 869 (1978).

[39] G. Herzberg, *Molecular Spectra and Molecular Structure*, Electronic Spectra and Electronic Structure of Polyatomic Molecules Vol. III (corrected reprint of 1966 edition) (Krieger, Malabar, FL, 1991.

[40] B. P. Winnewisser, in *Molecular Spectroscopy: Modern Research*, edited by K. N. Rao (Academic, Orlando, 1985), Vol. 3, p. 321, and references therein.

[41] A. F. Borro, I. M. Mills, and A. Mose, Chem. Phys. **190**, 363 (1995).

[42] V. Ahrens, F. Lewen, S. Takano, G. Winnewisser, Š. Urban, A. A. Negirev, and A. N. Koroliev, Z. Naturforsch. A **57**, 669 (2002).

[43] F. DeLucia and W. Gordy, Phys. Rev. **187**, 58 (1969).

[44] H. A. Bechtel, A. H. Steeves, and R. W. Field, Astrophys. J. **649**, L53 (2006).

[45] J. M. L. J. Reinartz, W. L. Meerts, and A. Dymanus, Chem. Phys. **31**, 19 (1978).

[46] D. H. Sutter and H. Dreizler, Z. Naturforsch. A **56**, 425 (2001).

[47] R. A. Forman and D. R. Lide, Jr., J. Chem. Phys. **39**, 1133 (1963).

[48] P. Pyykkö, Mol. Phys. **106**, 1965 (2008).

[49] C. H. Townes and B. P. Dailey, J. Chem. Phys. **17**, 782 (1949).

[50] B. P. Dailey, J. Phys. Chem. **57**, 490 (1953).

[51] I. Mills, T. Cvitaš, K. Homann, N. Kallay, and K. Kuchitsu, *Quantities, Units and Symbols in Physical Chemistry*, 2nd ed. (Blackwell Scientific Publications, Oxford, 1993).

[52] R. G. Gordon and J. K. Cashion, J. Chem. Phys. **44**, 1190 (1966).

[53] S. G. Kukolich, J. Chem. Phys. **50**, 3751 (1969).

[54] P. Thaddeus, L. C. Krisher, and J. H. N. Loubser, J. Chem. Phys. **40**, 257 (1964).

[55] W. L. Ebenstein and J. S. Muenter, J. Chem. Phys. **80**, 3989 (1984).

[56] H. A. Bechtel, A. H. Steeves, B. M. Wong, and R. W. Field, Angew. Chem., Int. Ed. Engl. **47**, 2969 (2008).

[57] T. van Mourik, G. J. Harris, O. L. Polyansky, J. Tennyson, A. G. Császár, and P. J. Knowles, J. Chem. Phys. **115**, 3706 (2001).

[58] G. Schaftenaar and J. H. Noordik, J. Comput.-Aided Mol. Des. **14**, 123 (2000).

[59] R. S. Mulliken, J. Chem. Phys. **23**, 1833 (1955).

[60] J. P. Foster and F. Weinhold, J. Am. Chem. Soc. **102**, 7211 (1980).

[61] R. F. W. Bader, *Atoms in Molecules: A Quantum Theory* (Oxford University Press, USA, 1994).

[62] B. M. Wong, Phys. Chem. Chem. Phys. **10**, 5599 (2008).